

PREDICTION OF PROCESS-INDUCED DEFORMATIONS USING DEEP LEARNING INTERFACED FINITE ELEMENT (FE) CONSTITUTIVE MODELS

Aravind Balaji¹, Claudio Sbarufatti², Antoine Parmentier³, David Dumas⁴ and Francesco Cadini⁵

¹ Cenaero Research Center, Rue des Frères Wright 29, 6041 Gosselies, Belgium, Email: aravind.balaji@polimi.it / aravind.balaji@cenaero.be, Website: <https://www.cenaero.be/>

² Department of Mechanical Engineering, Politecnico di Milano, via La Masa 1, 20156 Milan, Italy, Email: claudio.sbarufatti@polimi.it, Website: <https://www.polimi.it/>

³ Cenaero Research Center, Rue des Frères Wright 29, 6041 Gosselies, Belgium, Email: antoine.parmentier@cenaero.be, Website: <https://www.cenaero.be/>

⁴ Cenaero Research Center, Rue des Frères Wright 29, 6041 Gosselies, Belgium, Email: david.dumas@cenaero.be, Website: <https://www.cenaero.be/>

⁵ Department of Mechanical Engineering, Politecnico di Milano, via La Masa 1, 20156 Milan, Italy, Email: francesco.cadini@polimi.it, Website: <https://www.polimi.it/>

Keywords: Virtual Manufacturing, Process-induced deformations, Cure behaviour, Neural Network

ABSTRACT

The aim of the study is to improve the predictive capacity of a Finite Element tool in relation to a rheological thermo-chemo-viscoelastic constitutive model. This enhancement specifically focuses on accurately capturing the Process Induced Deformations (PID) resulting from the polymerization of thermoset composite matrix. These deformations are due to the internal residual stress that arises from the material's inherent anisotropic properties, specifically the coefficients of thermal expansion and chemical shrinkage. The focus of the study is to accurately model the cure polymerization behaviour, which is known to have a significant impact on manufacturing defects. To account for the effect of process variables, such as maximum curing temperatures and temperature rates, a non-parametric neural network model is implemented instead of a parametric diffusion cure-kinetics model. Such model is trained using Differential Scanning Calorimetry characterization tests and is interfaced with the classical visco-elastic constitutive model to predict the evolution of thermoset resin states, which is evaluated using two cure state variables: degree of cure and glass transition temperature. This improved prediction of state transitions results in precise evaluations of internal residual stresses, leading to accurate PID predictions. Anisotropic properties of carbon/epoxy woven composite at different states of cure are used for the numerical analyses. Finally, the enhanced methodology is applied to a case study of a Z-shaped thermoset part, and the predicted PID closely associates with the experimental measures.

1 INTRODUCTION

The aerospace industry has widely utilized thermosetting composite materials due to their high strength to weight ratio. However, it has been observed that multiple iterations are required to establish an efficient manufacturing process due to defects in the composite material (i.e., resin and fibre) and mould characteristics, as noted in [1-2]. During the manufacturing phase, composite parts undergo distortion and attain internal residual stresses as they are processed within the mould. Thus, it is crucial to have reliable numerical tools for designing and optimizing ideal manufacturing conditions to produce parts with fewer process-induced defects.

Various factors at different mechanical levels contribute to the development of manufacturing defects caused by internal residual stress, as discussed in [3-4]. The curing process of thermosetting resin, which undergoes transitions from viscous to rubbery to glassy states, leads to internal residual stresses and deformations due to the resin's thermal and chemical behaviour, [5]. Thermal stress fields arise from the difference in coefficients of thermal expansion (CTE) between the resin and the fibre, as demonstrated numerically, [6], and careful consideration of this property is necessary to minimize the

deformations in the final part. Chemical shrinkage associated with coefficients of chemical shrinkage (CCS) also contributes to residual stresses by reducing the free volume of the resin during the curing process, resulting in uniform tensile residual stresses distributed throughout the composite laminate, [7]. Deformations are additionally limited by contact with the mould during curing, further contributing to the development of internal residual stresses.

Finite Element (FE) analyses coupled with mechanical constitutive models is effective for analysing the different mechanisms during manufacturing, with various models implemented over the years, including elasticity and visco-elasticity. Although fully viscoelastic models provide accurate cure behaviour, they require extensive material characterization and come with high computational costs and memory requirements. The Cure Hardening Instantaneously Linear Elastic (CHILE) model provides a less complex alternative, with modulus changes as a function of cure state. However, modelling the evolution of cure state during manufacture remains a big question due to uncertainties in resin thermal history, formulations, and characterization boundary conditions and has received limited attention, [8-10].

In this study we propose to interface a non-parametric model with the user material subroutine of the numerical FE tool and hence, alleviating the burden associated with choice of cure-kinetics model and its optimized parameters. Moreover, accurate cure behaviour is modelled, leading to closer Process Induced Deformations (PID) predictions. Section 2 describes the theory and methodology associated with modelling of cure behaviour, the viscoelastic constitutive model, the Differential Scanning Calorimetry (DSC) characterization tests and the non-parametric neural network model. In Section 3, the performance of the non-parametric model is evaluated and a case study on PID prediction comparison for the case study of Z-shaped thermoset part using different constitutive models is made. Finally, in Section 4, the conclusions, and remarks from the study are summarized.

2 THEORY AND METHODOLOGY

2.1 Cure kinetics and associated state variables

The crucial properties relevant to the curing and modelling of residual stresses are a degree of cure, instantaneous glass transition temperature, expansional strains, coefficients of thermal expansion and chemical shrinkage and composite laminate properties. The degree of cure, X introduced previously is the ratio between heat released at a time over the total amount of heat released during the entire curing process. The cure kinetics model, [28] is implemented to describe the development of cure in terms of polymerization rate, which is given by,

$$\frac{dX}{dt} = \frac{K X^m (1-X)^n}{1 + e^{C(X-X_c)}} \quad (1)$$

$$\text{where, } K = Ae^{-\Delta E/RT} \text{ and } X_c = \iota_0 - (\iota_1 T)$$

where K is the rate constant, R is the molar gas constant, A is the exponential law coefficient, E is the activation energy, m and n are the first and second exponential constants, C is the diffusion constant, ι_0 is the critical X at the initial time and ι_1 is a constant accounting for the increase in X with temperature, T . The critical points in the cure evolution are X_{gel} and X_{vir} defining the transition between different material states. The transition from rubbery to glassy state is understood to occur when the process temperature matches with the instantaneous glass transition temperature, T_g which is defined as a function of degree of cure. The generic function used is the DiBenedetto's relationship, [11], which is given by,

$$\frac{T_g - T_{g\infty}}{T_{g\infty} - T_{g0}} = \frac{\lambda X}{1 - (1-\lambda)X} \quad (2)$$

T_{g0} and $T_{g\infty}$ are the glass transition temperature at the gel point and vitrification point respectively, and λ is the material dependent parameter when fitting equation to experimental measurements. The evolution of cure-state variables for a generic case of two-dwell Manufacturing Recommended Curing cycle (MRCC) with temperature rates, $r_{i=1,2,\dots,5}$ are shown in Fig. 1. The anisotropic properties associated with the material are different in different states and it is crucial to model such state transitions to predict the PID accurately.

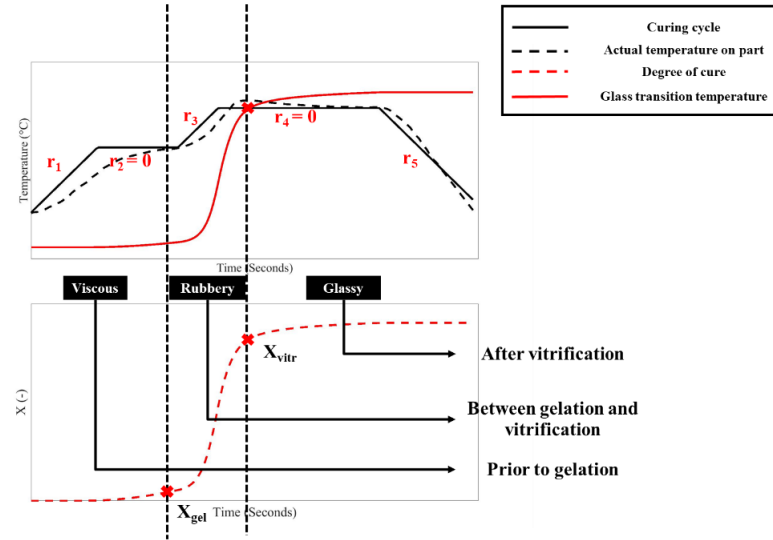


Figure 1: Evolution of cure state variables and a generic curing temperature cycle with associated process condition variables

2.2 Visco-elastic constitutive model

As anticipated in the introduction, the state-of-the-art solution for predicting the PID are FE tools with thermo-viscoelastic constitutive models. The common material behaviours used to assess the defects are the Cure Hardening Instantaneous Linear Elastic (CHILE) model and the non-linear viscoelastic model. The classic case of CHILE model proposed, [14-15] where a path dependence on cure state variables is exploited within the study. A model describing CHILE, or the non-linear viscoelastic behaviour of the partially cured resin, accounts for the curing temperature, instantaneous glass transition temperature and curing time. The instantaneous relaxation modulus corresponding to the Maxwell's element within the viscoelastic model of the partially cured resin is dependent on the reduced time, which is in turn dependent on the curing state variables. The thermo-viscoelasticity for anisotropic and thermo-chemo-rheological materials is simply written in integral form as a function of instantaneous relaxation modulus, C is given as,

$$\boldsymbol{\sigma}(t) = \mathbf{C}\boldsymbol{\varepsilon} + \int_0^t \delta\mathbf{C}(\boldsymbol{\psi} - \boldsymbol{\psi}') \frac{\partial(\boldsymbol{\varepsilon} - \boldsymbol{\varepsilon}^E)}{\partial\tau} \partial\tau \quad (3)$$

$$\mathbf{C} = \mathbf{C}_\infty + \sum_{n=1}^N \mathbf{C}_n e^{(-t/\rho^n)} \forall X \geq X_{gel} \text{ else } \mathbf{C} = 0 \quad (4)$$

where \mathbf{C} is the linear elastic Hooke tensor, $\delta\mathbf{C}$ is independent relaxation function for N Maxwell elements, $\boldsymbol{\varepsilon}^E$ is the expansional strain corresponding to thermal expansion and chemical shrinkage, \mathbf{C}_∞ is the fully relaxed modulus of uncured resin, \mathbf{C}_n are the spring constant, ρ^n are the relaxation times, $\boldsymbol{\psi}$ and $\boldsymbol{\psi}'$ are the reduced time corresponding to spring and dashpot dependent on the curing state variables

respectively and is defined as,

$$\psi = \int_0^t \frac{1}{a_T} dt' ; \psi' = \int_0^t \frac{1}{a_T} d\tau' \quad (5)$$

The term a_T corresponds to shift factor in the constitutive model and is assumed to be taken as a function approaching 0 and infinity in rubbery and glassy state, respectively. With this assumption, the Hooke tensor in the rubbery state is fully relaxed, i.e., $C_r = C_\infty$ while in the glassy state, the Hooke tensor is defined as $C_g = C_\infty + \sum_{n=1}^N C_n$. The stress field as a function cure state variables attained upon simplification of equations (3-5) is given by,

$$\sigma = \begin{cases} C_r(\boldsymbol{\varepsilon} - \boldsymbol{\varepsilon}^E), \forall T \geq T_g(X) \\ C_g(\boldsymbol{\varepsilon} - \boldsymbol{\varepsilon}^E) - (C_g - C_r)(\boldsymbol{\varepsilon} - \boldsymbol{\varepsilon}^E)|_{t=t_{vitr}}, \forall T < T_g(X) \end{cases} \quad (6)$$

The incremental stress state formulation of the equations (6) is implemented within the FE solver, [25]. Corresponding to the constitutive model, the material is assumed to be fully relaxed during the rubbery and viscous states. Meanwhile, the stress states within the glassy state are incrementally stored. Such ‘‘locked-in’’ stresses are finally releases upon demoulding and completion of curing process to give PID in form of distorted shapes.

2.3 Characterization tests and process conditions variables

Three DSC tests corresponding to temperature cycle at three different temperature rates, r at 1.5°C/min , 0.55°C/min and 0.5°C/min , with isothermal dwells at 180°C , 175°C and 185°C , respectively are studied for the epoxy resin carbon fibre, see Fig. 2. A few milligrams of the resin sample are subjected to the prescribed curing temperature cycle and the heat released by the sample during the curing process and the heat absorbed by the sample are recorded.

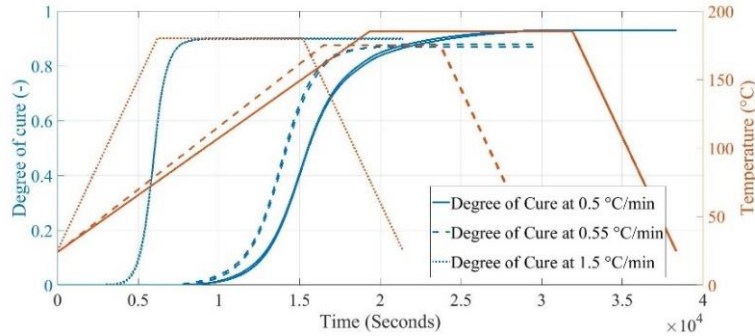


Figure 2 : Different curing conditions and its associated X

The enthalpy of reaction (during and at the end of cure cycle) and the residual enthalpy after the production cycle can be determined with such characterization test. The evolution of the resin reaction rate, $\frac{dX}{dt}$ as a function of time (and temperature) is the ratio of enthalpy during the reaction to the total reaction enthalpy, see Fig. 3.

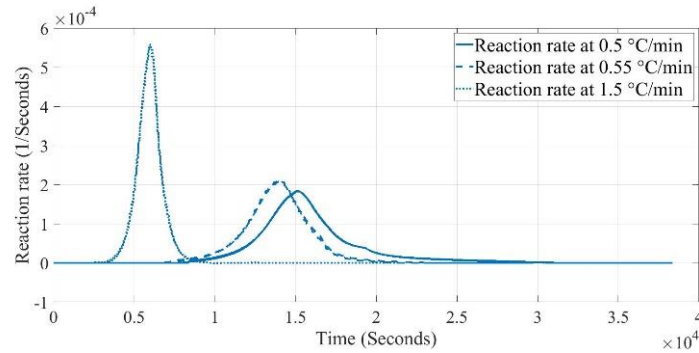


Figure 3: Different curing conditions and its associated $\frac{dX}{dt}$

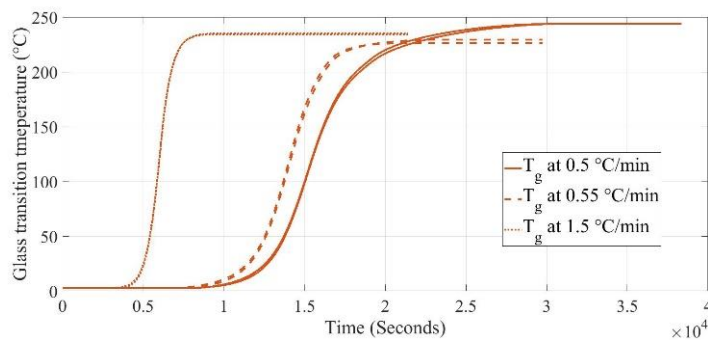


Figure 4: Different curing conditions and its associated T_g

In the early stages of the cure, the reaction rate is relatively slow due to the presence of unreacted functional groups within the resin. As the cure proceeds, the number of unreacted functional groups decreases, and the reaction rate increases. Moreover, the sample undergoes a change in heat capacity due to a change in its molecular mobility, which results in a characteristic step-change in the DSC curve. This step-change in heat capacity is used to determine the T_g of the material, refer Fig. 4. Eventually, the reaction rate slows down again as the resin approaches full cure. To confirm the residual cross-linking enthalpy and to be sure that the sample is cured completely, the test is performed again for the same cycles.

2.4 Non-parametric cure-kinetics model

To precisely model the curing behaviour, the cure state variables have been solved for each state separately in the recent past, [12]. However, this approach requires the use of a larger number of constants for modelling the cure behaviour. Alternatively, an efficient cure kinetics model which accounts this phenomenon with a help of diffusion control, [13] and is used for 8552/AS4 unidirectional composite material as introduced earlier. The diffusion cure-kinetics constants from [16] when implemented do not correlate accurately with the observed cure reaction rates at different process conditions and do not account for the process conditions variables. Moreover, the activation energy, E and reaction rate, m from equation (1) is observed to have influence on reaction rate peaks for the repeated tests on Hexcel RMT6 epoxy resin, [17]. Hence, there is a requirement to treat the model parameters stochastically to account for boundary condition uncertainties during curing process. Unfortunately, the lack of prior knowledge on model parameters for different resin poses challenges for stochastic simulations. Moreover, if the resin is expected to undergo significant changes in its chemical

composition, more complex cure kinetics formulations are required, [18-19].

Hence, there is need for simpler non-parametric models to predict the cure behaviour. Such model is introduced in form of neural networks, [20-22]. It is a supervised machine learning model which allows to capture the non-linear relationships between the input and the output variables without assuming a specific functional form like an Arrhenius model, refer equation (1). This makes it an efficient tool for predicting the cure kinetics and glass transition temperature of polymeric resin based on available DSC characterization tests. The neural network model is implemented to predict the $\frac{dX}{dt}$ and T_g , given the inputs, X , T and r at a given time. The model takes into consideration the different process conditions below 3 °C/min and maximum curing temperature of 180 °C with standard deviation of 4.47 °C. The architecture of the proposed model is shown in Fig. 5.

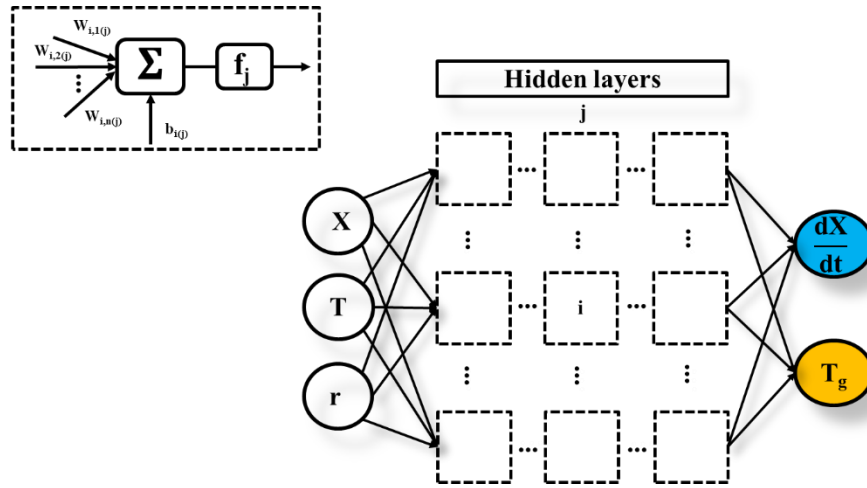


Figure 5: Non-parametric neural network architecture for predicting cure state variables. The i^{th} neuron in the j^{th} hidden layer with its associated weights, biases, and activation function is shown.

Each of the three DSC tests consists of data samples of which 75%, 15% and 10% are used for training, validating, and testing the neural network model respectively. The normalization of these input features between 0 and 1 is done to associate similar weights and this, in turn accelerates the training algorithm. The network characteristics are derived by employing a training algorithm that utilizes a gradient descent approach to minimize the error between the network's predictions and the expected outputs obtained from the second set of DSC tests conducted under the same curing boundary conditions. The minimization function is executed with respect to the vector, containing the weights and biases. The characteristics of the optimized neural network model are given in Table 1. The model is used instead of parametric diffusion cure-kinetics and DiBenedetto's models, considering the dependency on the process condition variables.

Network structure	Activation functions	RMSE
3-13-13-2	Sigmoid (Hidden layers, $f_{i=1,2}$) Linear (Output layer, f_3)	Training set (0.9952) Validation set (0.9929) Test set (0.9944)

Table 1: Optimized non-parametric neural network characteristics

3 RESULTS AND DISCUSSIONS

3.1 Performance of the non-parametric neural network model

Comparison of predictions between neural network and diffusion cure-kinetics models is shown in Fig. 6. Authors of [23] implemented the diffusion cure-kinetics model with adjusted model parameters. These were determined using a regression procedure to minimize the error between experimental data and model predictions, in the least squares sense. Three pairs of additional DSC tests based on pure resin and on epoxy resin carbon fibre subject to partial curing temperature cycles were used for such procedure in addition to the existing dataset. The peak and post summit regime of the $\frac{dX}{dt}$ evolution, in the case of a 1°C/min temperature rate with an isothermal dwell at 180 °C, [26-27] shows a closer correlation to experimental measurements according to the non-parametric neural network model. While the parametric model captures the cure behaviour with less accuracy, a trained neural network-based model is observed to be the better choice due to its capability of handling non-linear relationships accurately at different boundary conditions. This allows to model the thermo-chemical analysis accurately because of process variables uncertainties on the thermoset part which is in turn dependent on factors such as part thickness, rate of polymerization and heat transfer coefficient of the oven. This is applicable in scenario as shown in Fig. 1 where the actual temperature profile is different from the control cure temperature with modified temperature rates.

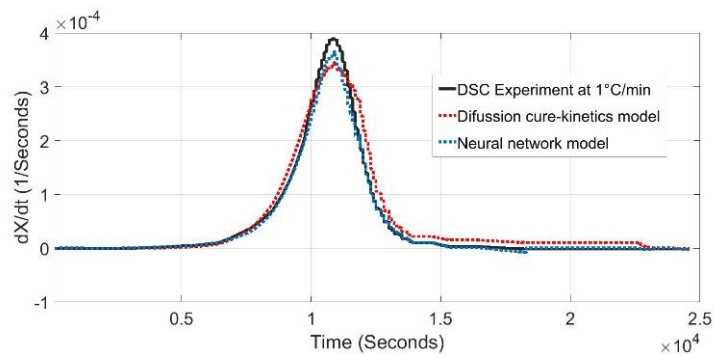


Figure 6: Comparison of performance of neural network interfaced and diffusion cure-kinetics interfaced models to predict the evolution of reaction rate, $\frac{dX}{dt}$ for the case of $r = 1 \text{ }^\circ\text{C}/\text{min}$, with isothermal dwell at 180 °C

3.2 Case Study: Numerical analysis on PIDs of Z-shaped thermoset part

The materials of interest are the unidirectional and woven carbon/epoxy prepregs AS4/8552 produced by Hexcel, [24]. A Z-shaped part consisting of a stacking sequence, $[\pm 45^\circ/0-90^\circ]_{4s}$ made of 15 plies are manufactured on an Invar mould with a negligible coefficient of thermal expansion. The geometry of Z-shaped part is as shown in Fig. 7. The part is 3 mm thick and 150 mm long in Z-axis. Cure cycle applied in numerical analysis comprises of a heating ramp with temperature rate of 1.5 °C/min from room temperature to 180 °C. The part is maintained at an isothermal dwell at this 180 °C for 120 minutes before cooling back to the room temperature with rate of 2 °C/min. A pressure of 7 bars is applied on Z-shaped part throughout whole duration of cure cycle. An autoclave boundary condition is adopted to mimic the real experimental scenario more closely, where pressure is applied to keep the part in place against the mould, preventing the free closure of curved sections in the Z-part. The X, Y, and Z in the local coordinate system of the FE model indicate the warp, weft, and through thickness directions, respectively. The thickness, and orientations of the plies are specified, and the draping process is modelled using the Simulayt Composite Modeller. Subsequently, to achieve the 3D geometrical representation, the defined shell geometry is extruded and meshed in the thickness direction.

The numerical model consists of a 3D representation of the part, comprised of 19665 hexahedral C3D8 elements with linear geometry and assigned local orientations. The mould, on the other hand, is represented as a rigid component, using 2296 quadrilateral R3D4 elements with linear geometry.

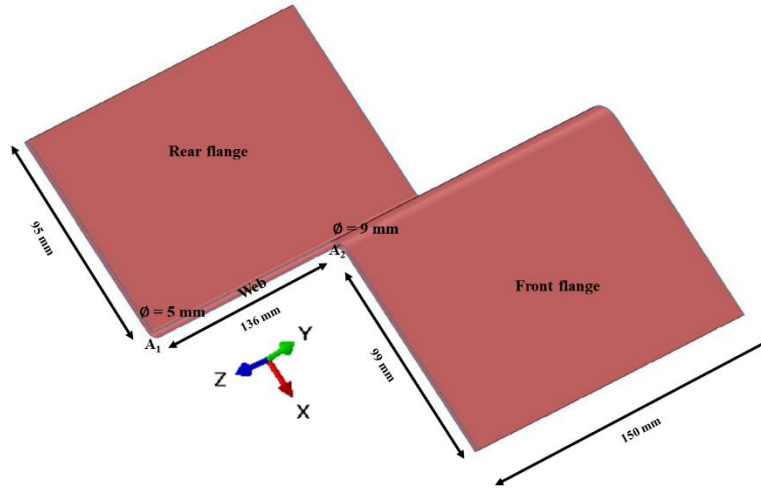


Figure 7: 3D geometry of the Z-shaped thermoset 8552/AS4 part

In the FE constitutive model, the thermosetting material's behaviour is assumed to be orthotropic, and the material properties are considered constant for every state during the curing process. The resin fibre woven matrix is assumed to be homogeneous at ply-scale level and the orthotropic properties are listed in Table 2, [23]. The Z-shaped part is produced using an Invar tool which has a negligible CTE. Additionally, a frictionless contact condition is assumed between the part and the tool. The numerical FE analysis follows a linear viscoelastic constitutive model with superposition between cure state variables and process conditions.

Properties	SI Unit	Rubbery state	Glassy state
Modulus in warp and weft direction	MPa	66190	68000
Through thickness Modulus	MPa	165	10000
In plane shear Modulus in off-axis direction	MPa	44.3	5000
Out of plane shear Modulus	MPa	42.9	4500
In plane (between warp and weft direction) Poisson's ratio	-	0.001	0.220
Out of plane (between warp and through thickness direction) Poisson's ratio	-	0.002	0.072
Out of plane (between weft and through thickness direction) Poisson's ratio	-	0.833	0.490
CTE in warp and weft directions	1/°C	-7.11×10^{-7}	2.50×10^{-7}
CTE in through thickness direction	1/°C	3.5×10^{-4}	5.88×10^{-4}
CCS in warp and weft directions	-	9.31×10^{-4}	5.29×10^{-4}
CCS in through thickness direction	-	-3.45×10^{-2}	-2.53×10^{-2}

Table 2: Anisotropic properties associated with 8552/AS4 material with fibre volume fraction of 60% at different states

Fig. 8 illustrates the comparison of residual stress field in X direction between neural network and diffusion cure-kinetics interfaced constitutive models. The stress field before the cooling phase, after the cooling phase and upon de-moulding are compared. The variation in localized stress fields within the curved sections prior to the cooling phase is approximately between 42% to 44%. Such differences in numerical predictions relies on accurate modelling of the cure behaviour.

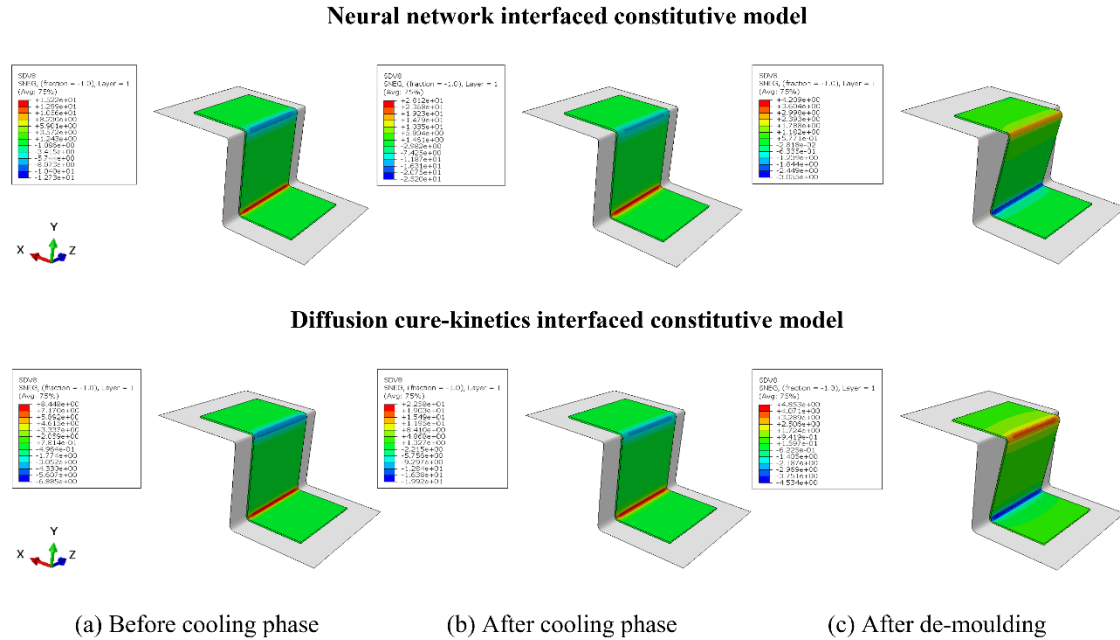


Figure 8: Comparison of residual stress in the X axis (scaling deformation factor: 5.0)

The evolution of expansional strains on an element of the front flange in Z-shaped part during the curing process are illustrated in Fig. 9. According to equation (6), during the rubbery state, the constitutive model assumes the material to be fully relaxed. Hence, the "locked-in" residual stresses developed is released to attain deformation during the cure. On the other hand, in the glassy state, the "locked-in" residual stress is stored incrementally and released upon de-moulding. The percentile difference in strain in the warp and through thickness directions with new approach upon de-moulding over the curing process is 16.98% because of earlier onset of vitrification phenomenon. This generates additional stresses which eventually is released to attain the PID in form of spring-in angles A_1 and A_2 .

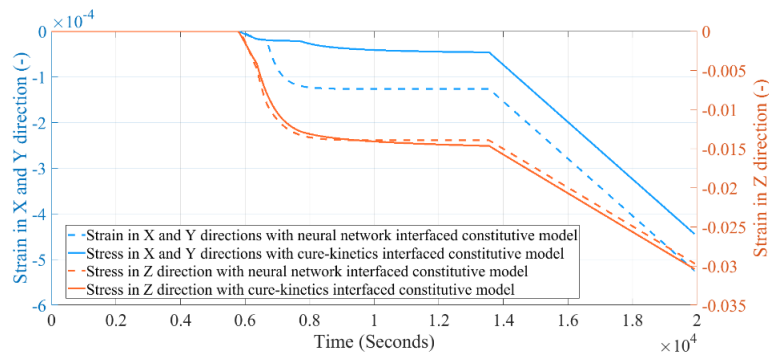


Figure 9: Comparison of strains in the warp, weft, and through-thickness directions on the flange of Z-shaped part

Validation of the internal residual stress field is achieved through a comparison of process induced defects. The experimental measurement of process induced defects using the laser scanner and subsequent analysis of the point clouds can provide valuable information on the quality and accuracy of the manufacturing process. With the case study, process induced defects in form of spring-in angles were measured using the point clouds acquired with Nikon MMDx100 laser scanner subject to post-processing, [23]. These points are used to determine a map of deviations between the initial reference and distorted geometry. Such experimental measures are acquired with 0.2° standard deviation. Comparison of spring-in angles, A_1 and A_2 post de-moulding between the viscoelastic models interfaced with cure-kinetics model and neural network model is shown in Fig. 10.

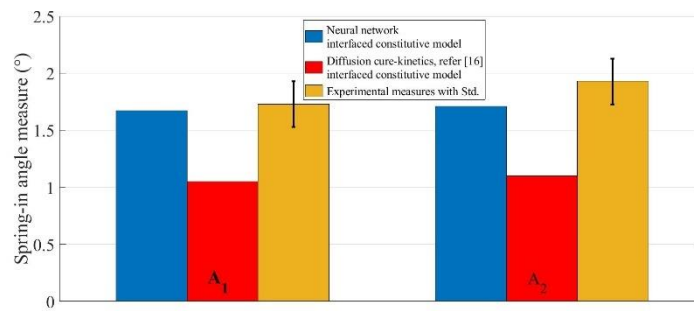


Figure 10: PID prediction (spring-in angle measure) comparisons

With the PID predictions in form of spring-in angles on the curved sections, the proposed numerical analysis gives closer prediction with difference of 3.46 % for angle A_1 (fibre-rich zone) in comparison to difference of 11.39 % for angles A_2 (resin-rich zone). The computational costs and memory requirement with the proposed approach is fractionally higher (1.08 times) because of non-linearity of activation functions associated with the neural network model.

4 CONCLUSIONS

Defects and internal residual stress unavoidably occur during manufacturing, attributed to the thermal expansion and chemical shrinkage phenomenon associated with thermoset materials. Hence, it is essential to accurately model the cure behaviour to minimize PID and ensure the production of high-quality thermoset composite parts. In this study, a numerical model is utilized to examine the residual stress fields in a thermosetting composite under autoclave boundary conditions. The model relies on accurately capturing the transitions between the viscous, rubbery, and glassy states, considering the cure behaviour of the resin and fibre. To capture the complex and non-linear relationships between cure kinetics and process variables, a non-parametric neural network model is employed.

The study provides insights into the influence of process temperature rates (below $3^\circ\text{C}/\text{min}$) on the evolution of cure state parameters for a specific woven carbon/epoxy prepreg, AS4/8552. Additionally, the non-parametric model is integrated with the viscoelastic constitutive model to make precise predictions of process-induced defects in the form of spring-in angles. Furthermore, the study offers a deeper understanding of the nature of the residual stress field in the case of a Z-shaped thermoset part. This modelling approach proves particularly useful when dealing with thick thermosets experiencing different temperature gradients between the control temperature and the part temperature.

The information obtained from the neural network-interfaced constitutive model and the validated

residual stress field can be applied in damage propagation analyses, enabling further enhancements in the manufacturing process. This approach provides an initial accurate estimation of defects and facilitates the optimization of temperature profiles to reduce risks and enhance manufacturing quality.

ACKNOWLEDGEMENTS

This project has received funding from the European Union's Horizon 2020 research and innovation programme under the Marie Skłodowska-Curie grant agreement no. 859957.

REFERENCES

- [1] S.G. Advani and E.M. Sozer, *Process Modeling in Composites Manufacturing*, (1st ed.), CRC press, 2003.
- [2] J.M. Svanberg, *Predictions of manufacturing induced shape distortions: high performance thermoset composites*, Doctoral thesis, Luleå University of Technology, 2002.
- [3] P. P. Parlevliet, H. E. N. Bersee and A. Beukers, Residual stresses in thermoplastic composites- A study of the literature-Part I: Formation of residual stresses, *Composites Part A: Applied Science and Manufacturing*, **37(11)**, 2006, pp. 1847-1857 (doi: [10.1016/j.compositesa.2005.12.025](https://doi.org/10.1016/j.compositesa.2005.12.025)).
- [4] N. Zobeiry and A. Poursartip, The origins of residual stress and its evaluation in composite materials, *Structural Integrity and Durability of Advanced Composites: Innovative Modelling Methods and Intelligent Design*, 2015, pp. 43-71 (doi: [10.1016/B978-0-08-100137-0.00003-1](https://doi.org/10.1016/B978-0-08-100137-0.00003-1)).
- [5] J. Lange, S. Toll, J. A. E. Månson and A. Hult, Residual stress build-up in thermoset films cured above their ultimate glass transition temperature, *International Journal of Solids and Structures*, **36(16)**, 1995, pp. 3135-3141 (doi: [10.1016/S0032-3861\(96\)00584-8](https://doi.org/10.1016/S0032-3861(96)00584-8)).
- [6] P. Prasatya, G. B. McKenna and S. L. Simon, A Viscoelastic Model for Predicting Isotropic Residual Stresses in Thermosetting Materials: Effects of Processing Parameters, *Journal of Composite Materials*, **35(10)**, 2001, pp. 826-848 (doi: [10.1106/D0JJ-V6Q1-891M-3GJR](https://doi.org/10.1106/D0JJ-V6Q1-891M-3GJR)).
- [7] T. A. Bogetti and J. W. Gillespie, Process-Induced Stress and Deformation in Thick-Section Thermoset Composite Laminates, *Journal of Composite Materials*, **26(5)**, 1992, pp. 626-660 (doi: [10.1177/002199839202600502](https://doi.org/10.1177/002199839202600502)).
- [8] T. S. Mesogitis, A. A. Skordos and A. C. Long, Uncertainty in the manufacturing of fibrous thermosetting composites: A review, *Composites Part A: Applied Science and Manufacturing*, **57**, 2014, pp. 67-75 (doi: [10.1016/j.compositesa.2013.11.004](https://doi.org/10.1016/j.compositesa.2013.11.004)).
- [9] F-L. Jin, X. Li and S-J. Park, Synthesis and application of epoxy resins: A review, *Journal of Industrial and Engineering Chemistry*, **29**, 2015, pp. 1-11 (doi: [10.1016/j.jiec.2015.03.026](https://doi.org/10.1016/j.jiec.2015.03.026)).
- [10] D. Dykeman, *Minimizing uncertainty in cure modeling for composites manufacturing*, Doctoral Thesis, The University of British Columbia, Vancouver, 2008.
- [11] H. Stutz, K. H. Illers and J. Mertes, A generalized theory for the glass transition temperature of crosslinked and uncrosslinked polymers, *Journal of Polymer Science: Part B: Polymer Physics*, **28(9)**, 1990, pp. 1483-1498 (doi: [10.1002/POLB.1990.090280906](https://doi.org/10.1002/POLB.1990.090280906)).
- [12] L. Sun, S. Pang, A. M. Sterling and I. I. Negulescu and M. A. Stubblefield, Dynamic Modeling of Curing Process of epoxy Prepreg, *Journal of Applied Polymer Science*, **86**, 2002, pp. 1911-1923 (doi: [10.1002/app.11146](https://doi.org/10.1002/app.11146)).
- [13] D. J. O'Brien, P. T. Mathe and S. R. White, Viscoelastic Properties of an Epoxy Resin during Cure, *Journal of Composite Materials*, **35(10)**, 2001, pp. 883-904 (doi: [10.1177/a037323](https://doi.org/10.1177/a037323)).
- [14] D. Adolf and J. E. Martin, Time-cure superposition during crosslinking, *Macromolecules*, **23(15)**, 1990, pp. 3700-3704 (doi: [10.1021/ma00217a026](https://doi.org/10.1021/ma00217a026)).

- [15] J.M. Svanberg and J.A. Holmberg, Prediction of shape distortions Part I. FE-implementation of a path dependent constitutive model, *Composites part A: Applied science and manufacturing*, **35**(6), 2004, pp. 711-721 (doi: [10.1016/j.compositesa.2004.02.005](https://doi.org/10.1016/j.compositesa.2004.02.005)).
- [16] N. Ersoy, K. Potter, M. R. Wisnom and M. Clegg, Development of spring-in angle during cure of a thermosetting composite, *Composites Part A: Applied Science and Manufacturing*, **36**(12), 2005, pp. 1700-1706 (doi: [10.1016/j.compositesa.2005.02.013](https://doi.org/10.1016/j.compositesa.2005.02.013)).
- [17] T. S. Mesogitis, A. A. Skordos and A. C. Long, Stochastic simulation of the influence of cure kinetics uncertainty on composites cure, *Composites Science and Technology*, **110**, 2015, pp. 145-151 (doi: [10.1016/j.compscitech.2015.02.009](https://doi.org/10.1016/j.compscitech.2015.02.009)).
- [18] G. Voto, L. Sequeira and A. A. Skordos, Formulation based predictive cure kinetics modelling of epoxy resins, *Polymers*, **236**, 2021 (doi: [10.1016/j.polymer.2021.124304](https://doi.org/10.1016/j.polymer.2021.124304)).
- [19] L. A. Strömbeck and B. R. Gebart, Optimization of cure kinetics model parameters from DSC-data, *Thermochimica Acta*, **214**(1), 1993, pp. 145-148 (doi: [https://doi.org/10.1016/0040-6031\(93\)80049-G](https://doi.org/10.1016/0040-6031(93)80049-G)).
- [20] S. Haykin, *Neural networks: a comprehensive foundation*, Vol. 2, Prentice Hall, 1998.
- [21] C. M. Bishop, *Neural network for pattern recognition*, Oxford University press, Oxford, 1995.
- [22] C. M. Bishop, *Pattern recognition and machine learning*, Springer, 2006.
- [23] A. Parmentier and B. Wucher and D. Dumas, Determination of the model complexity level required to predict the cure-induced deformations in thermoset-based composite parts, *ECCM16-16th European Conference on Composite Materials, Seville, Spain, June 22-26, 2014*, Seville, 2014.
- [24] Hexcel, *Hexply 8552 product data sheet*, 2016, (URL: https://www.hexcel.com/user_area/content_media/raw/AS4_HexTow_DataSheet.pdf).
- [25] M. A. Zocher, S. E. Groves and D. H. Allen, A three-dimensional finite element formulation for thermoviscoelastic orthotropic media, *International Journal for Numerical Methods in engineering*, **40**(12), 1997, pp. 2267-2288 (doi: [10.1002/\(SICI\)1097-0207\(19970630\)40:12<2267::AID-NME156>3.0.CO;2-P](https://doi.org/10.1002/(SICI)1097-0207(19970630)40:12<2267::AID-NME156>3.0.CO;2-P)).
- [26] D. V. Ee and A. Poursartip, *Hexply 8552 material properties database for use with compro cca and raven*, National Center for Advanced Materials Performance, Wichita, KS, 2009.
- [27] A. Shahkarami, D. V. Ee and A. Poursartip, *Material characterization for processing: Hexcel 8552*, National Center for Advanced Materials Performance, Wichita, KS, 2009.
- [28] K. C. Cole and J. J. Hechler and D. Noel, A new approach to modeling the cure kinetics of epoxy/amine thermosetting resins. 2. Application to a typical system based on bis[4-(diglycidylamino)phenyl]methane and bis(4-aminophenyl) sulfone, *Macromolecules*, **24**(11), 1991, pp. 3098-3110 (doi: [10.1021/ma00011a012](https://doi.org/10.1021/ma00011a012)).